J Mater Sci (2010) 45:2715–2724
DOI 10.1007/s10853-010-4257-2

Use of analytical techniques for identification of inorganic polymer gel composition

D. Zaharaki · K. Komnitsas · V. Perdikatsis

Received: 27 October 2009 / Accepted: 20 January 2010 / Published online: 3 February 2010

Abstract In the present experimental study, a number of analytical techniques were used to identify the composition of gel and thus elucidate to a certain extent the mechanisms involved during synthesis of inorganic polymers. The raw materials used, low calcium slag from a ferronickel plant and commercial glass, were alkali activated by Na_2SiO_3 and KOH solutions. X-ray diffraction (XRD) is used to identify new formed phases; deconvolution of the amorphous peaks in X-ray powder diffraction patterns enables the quantitative estimation of the amorphous phases present. The morphology and composition of the inorganic polymer gel may be defined by optical reflection microscopy (ORM) and scanning electron microscopy (SEM). Fourier transform infrared spectroscopy (FTIR) is a useful tool for the identification of specific molecular structures including Si–O–Si and Al–O bonds, which define the degree of polysialation. Thermogravimetric analysis (TG) determines water evaporation rates in inorganic polymer structures by recording the weight loss under controlled heating. Finally, the effect of the presence in the starting mixture of heavy metals such as Pb or Cu and anions such as NO_3^- or SO_4^{2-} on the quality of the gel formed and subsequently on the compressive strength of inorganic polymers are studied and discussed.

Introduction

Inorganic polymers (geopolymers) are amorphous materials consisting of a network of SiO_4 and AlO_4 tetrahedra linked alternately by sharing all oxygen atoms. Their synthesis involves reactions between aluminosilicate powder and concentrated caustic alkali metal silicate solution yielding at ambient temperature tri-dimensional poly-sialates [1, 2].

The nature and characteristics of the raw materials used affect microstructure and properties of the gel formed and subsequently of inorganic polymers. Kaolinite and other clays have been used as fillers for the encapsulation of hazardous wastes and/or the manufacture of inorganic polymeric products [3, 4]. In the last decade, various wastes such as fly ash and slag have been studied as raw materials for the synthesis of inorganic polymers so that high added value products or structures for adequate immobilization of toxic and radioactive elements are produced [5–9].

Inorganic polymers exhibit excellent physical and chemical properties such as high compressive strength, low permeability (10^{-9} cm/s), acid and freeze–thaw resistance, thermal stability, etc. [10–12]. Potential applications of the inorganic polymers produced under alkali-activation include amongst others building materials, temperature stable resins for moulds, encapsulation of toxic wastes, surface capping of waste dumps, construction of low permeability base liners in landfills as well as stabilization of tailing dams [5, 13–15].

The exothermic process of inorganic polymer synthesis starts with the dissolution of raw materials exhibiting different degree of reactivity in alkaline solutions, the release of Si and Al ions and the formation of a $M_x(AlO_2)_y(SiO_2)_z{\cdot}n\text{MOH}{\cdot}m\text{H}_2\text{O}$ gel (M: K^+ or Na^+) that hardens quickly. The extent of dissolution of aluminosilicate materials, the degree of polymerization of the dissolved species and the resulting molar ratios between Na_2O, Al_2O_3 and SiO_2 control transformations from crystalline to

D. Zaharaki · K. Komnitsas (✉) · V. Perdikatsis
Department of Mineral Resources Engineering, Technical University of Crete, 73100 Hania, Greece
e-mail: komni@mred.tuc.gr

amorphous phase affecting thus the strength of the final products; the required time depends on synthesis conditions [16].

The degree of polymerization of silicate species in activating solutions is affected by alkalinity. KOH solution is used to dissolve and activate the surface of the raw material so that soluble silicate monomers are produced. When high concentrations of KOH are used, the number of silicates present in the system increases, thus increasing the rate of polymerization and inorganic polymer gel formation [17, 18]. Water also plays an important role in the entire process of inorganic polymer synthesis, however, high *L/S* ratios hinder polycondensation [19].

Addition of compounds containing cations such as aluminium, silicon, calcium or iron may affect negatively the mechanical properties of the inorganic polymers due to insufficient development of the three-dimensional polymeric aluminosilicate network. Due to the complex nature of most raw materials present in the starting mixture, the exact mechanisms that control synthesis of inorganic polymers namely dissolution, transportation or orientation and polycondensation, need to be further elucidated [20–22].

In the present experimental study, several analytical techniques, namely X-ray diffraction (XRD), optical reflection microscopy (ORM), scanning electron microscopy (SEM), Fourier transform infrared spectroscopy (FTIR) and Thermogravimetric analysis (TG) were used to identify the composition of gel and thus elucidate to a certain extent the mechanisms involved during synthesis of inorganic polymers when low calcium ferronickel slag and commercial glass are used as raw materials and Na_2SiO_3 and KOH as activating solutions. Also, the effect of the presence in the starting mixture of heavy metals such as Pb or Cu and anions such as NO_3^- or SO_4^{2-} on the quality of the gel formed is studied and discussed.

Experimental

The raw materials used are electric arc slag and/or commercial glass. Slag is produced at the LARCO S.A. ferronickel plant in Greece; 30% of it is used in the cement industry whilst the remaining volumes are disposed of in a nearby bay causing several environmental problems. The particle size of the as-received brittle slag which is cooled at the plant with the use of seawater varies between 0.075 and 4 mm. Olivines (fayalite and forsterite), anorthite, quartz, tridymite, cristobalite, magnetite and chromite are the main mineralogical phases present while its amorphous content exceeds 50%. Commercial glass is an amorphous material consisting mainly of silicon, calcium and sodium oxides.

Table 1 Chemical analysis of raw materials

%	Slag	Glass
$Fe_2O_{3(tot)}$	43.83	0.84
SiO_2	32.74	81.57
Al_2O_3	8.32	0.50
CaO	3.73	8.52
Cr_2O_3	3.07	–
MgO	2.76	0. 30
MnO	0.41	–
Na_2O	–	6.29
K_2O	–	0.40
P_2O_5	–	0.38
TiO_2	–	0.13
SO_3	–	0.08
S	0.18	–
C	0.11	–
Ni	0.10	–
Co	0.02	–
Total	95.27	99.01

Table 1 shows the chemical composition of slag and glass in the form of oxides and trace elements. Both materials were dried and crushed (slag: −120 μm and d_{50} −12 μm, glass: −350 μm and d_{50} −23 μm) using a FRITSCH pulverizer. Increased surface area usually improves the compressive strength of the produced inorganic polymers [23, 24]. Kaolinite (Fluka) was used as an additive in some cases.

The activating solution consists of a mixture of potassium hydroxide and sodium silicate (Merck, Na_2O:-$SiO_2 = 0.3$) solutions; for the preparation of KOH solution anhydrous pellets (ACS-ISO for analysis) were dissolved in distilled water. Raw materials were slowly added in solution under continuous mechanical mixing so that a homogeneous paste was obtained. The wt% addition of raw materials in solution varies and depends on the reagents used in each case to produce a workable paste.

The paste was cast in plastic cubic moulds (5 cm each side) which were vibrated for 5 min to eliminate the formation of air voids. Some specimens were pre-cured at room temperature for 2 days and then heated in a laboratory oven (MMM GmbH) at 80 °C for 48 h. After de-moulding, ageing took place at room temperature for 7 days in order to enhance the development of structural bonds. The compressive strength was then measured using an MTS 1600 load frame. All experiments were carried out in duplicate.

X-ray diffraction (XRD) analysis of the specimens was performed by a Siemens D500 diffractometer using a Co tube and a scanning range from 3° to 70° 2θ with a step 0.03° and 4°s/step measuring time. Qualitative analysis

was carried out using the Diffrac$_{plus}$ Software (Bruker AXS) and the PDF database. Imaging of the inorganic polymer morphology was carried out using a POL JENALAB Aus Jena polarized light microscope interfaced with a camera. Polished sections and thin polished sections were prepared and studied in polarizing microscope with low magnification up to ×200. A JEOL JSM-5400 scanning electron microscope equipped with an Oxford energy dispersive X-ray spectrometer (EDS) was used; samples were coated with carbon prior to analysis to increase conductivity of the surface. FTIR analysis was carried out by FTIR Spectrometer (Perkin-Elmer, Model 1000) using the KBr pellet technique (each sample was mixed with KBr at a ratio 1:100). TG analysis was performed using a Perkin Elmer Thermogravimetric Analyser TGA 6; samples were heated up to 700 °C at a rate of 10 °C min^{-1} using a nitrogen purge rate of 60 mL min^{-1}.

Sulphates or nitrates salts of Pb or Cu (0.5-3% w/w) were added in the starting mixture of slag-based inorganic polymers to assess the effect of the corresponding heavy metals and anions on the quality and the characteristics of the formed gel and subsequently on the compressive strength acquired; code numbers of the specimens produced in duplicates are seen in Table 2.

Results and discussion

XRD analysis

Figure 1 shows the XRD patterns of 94%–6% w/w slag–kaolinite (SK80) and 50%–50% w/w slag–glass (SG80) inorganic polymers. New formed phases include hydroxysodalite, maghemite, calcite, calcium silicate hydrates and trona. Quartz—SiO_2, fayalite—Fe_2SiO_4 and magnetite—Fe_3O_4 are phases that are also seen in the as-received slag. The presence of kaolinite in inorganic polymer SK80 indicates that the initially used quantity has not fully reacted during synthesis [21, 25].

Hydroxysodalite $Na_8Al_6Si_6O_{24}(OH)_2(H_2O)_2$, may be formed according to reaction (1) when NaOH reacts with kaolinite and OH^- replaces Cl^- ions in the framework of sodalite $Na_4Al_3(SiO_4)_3Cl$ [26, 27]. The dissolution of kaolinite provides OH^- and accelerates reaction (1), even at low-temperature hydrothermal conditions [28, 29]. Hydroxysodalite (or K-doped sodalite) may be formed in lesser quantities in SK80 and SG80 inorganic polymers.

$$3Al_2(Si_2O_5)(OH)_4 + 8NaOH \rightarrow Na_8Al_6Si_6O_{24}(OH)_2(H_2O)_2 + 7H_2O \quad (1)$$

Maghemite γ—Fe_2O_3, may be formed during low-temperature oxidation of ferrous iron phases present in the initial slag [30]. Calcite ($CaCO_3$), is formed when calcium hydroxide reacts with atmospheric carbon dioxide. Calcium silicate hydrated phases may be formed due to the presence of silicon and calcium in gel. Trona $Na_3(CO_3)(HCO_3)\cdot 2(H_2O)$ which belongs to soda minerals group and seen at the surface of both specimens may be formed according to reaction (2)

$$3NaOH + 2CO_2 + H_2O \rightarrow Na_3(CO_3)(HCO_3)\cdot 2H_2O \quad (2)$$

The broad peak seen between 27° and 42° 2θ in Fig. 1 for both specimens indicates a significant degree of amorphicity. The compressive strength acquired for inorganic polymers SK80 and SG80 reaches 40 and 47 MPa, respectively; it is known that higher amorphicity results in higher strength. The amorphicity of the specimens is more clearly seen in Fig. 2 where the XRD patterns of commercial glass and glass-based inorganic polymer G80 are presented. The broad peak seen for the initial glass between 17° and 34° 2θ is typical for amorphous phases; this peak is slightly shifted to the right (between 22° and 34° 2θ) for inorganic polymer G80 due to overlapping of the original glass-peak and the amorphicity of the specimen. Pirssonite [$CaNa_2(CO_3)_2(H_2O)_2$], which is detected in G80 specimen, is an evaporite formed as a result of atmospheric carbonation of glass.

Figure 3 shows the XRD pattern of inorganic polymer G80 in relation to glass and inorganic polymer amorphicity, after deconvolution of the original 2θ peaks 22.78° for glass and 29.65° for G80. "F1a" is the XRD pattern of inorganic polymer G80 also seen in Fig. 2, from 15° to 43° 2θ, calculated using the Eva diffrac^{plus} software. "F1b" which is the theoretical calculated curve is identical with "F1a". Curves "F2a" and "F2b" are almost identical indicating that practically no difference is seen between

Table 2 Code numbers of inorganic polymers synthesized with the addition of Pb or Cu as sulphate or nitrate salts

Code no.	Addition percentage of Pb or Cu	Max compressive strength, MPa (Code no.)
PBS05-PBS3	0.5–3% w/w Pb as $PbSO_4$	50.5 (PBS05)
PBN05-PBN3	0.5–3% w/w Pb as $Pb(NO_3)_2$	45.5 (PBN05)
CUS05-CUS3	0.5–3% w/w Cu as $CuSO_4\cdot 5H_2O$	32.2 (CUS05)
CUN05-CUN3	0.5–3% w/w Cu as $Cu(NO_3)_2\cdot 3H_2O$	26.0 (CUN05)

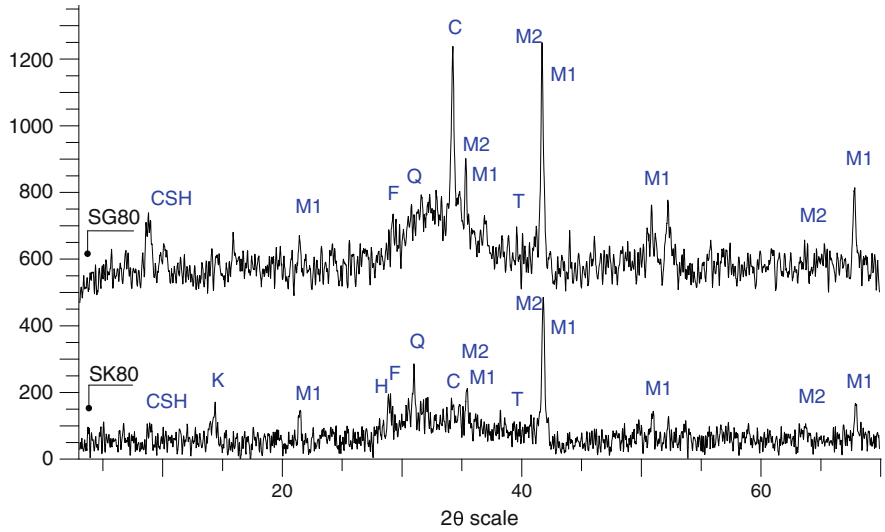

Fig. 1 XRD patterns of slag–kaolinite (SK80) and slag–glass inorganic polymers (SG80) (*Q* quartz, *K* kaolinite, *F* fayalite, *M1* magnetite, *M2* maghemite, *C* calcite, *H* hydroxysodalite, *T* trona, *CSH* calcium silicate hydrated phases)

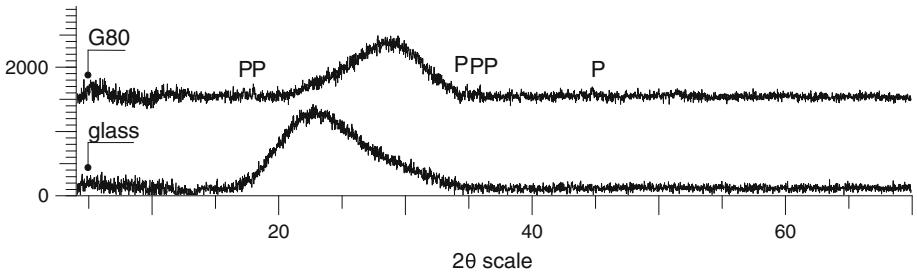

Fig. 2 XRD patterns of commercial glass and glass-based inorganic polymer (G80) (*P* pirssonite) [34]

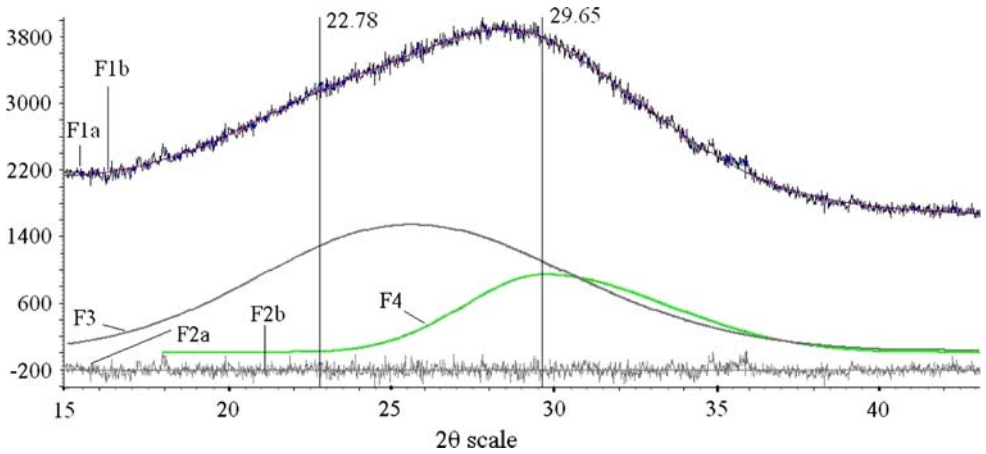

Fig. 3 XRD pattern of inorganic polymer G80 in relation to glass and inorganic polymer amorphicity

experimental and theoretical values. The profile refinement index R_p (= $\Sigma|y_{exper} - y_{theor}|/\Sigma y_{exper}$) is 1.65% while the respective weighted index R_{wp} is 2.11% indicating thus very good fit of experimental and theoretical profiles.

F3 and F4 are the peaks for glass and inorganic polymer after deconvolution carried out using the Software TOPAS (Brucker). By assuming that glass and inorganic polymer have similar mass absorption coefficients their quantitative composition can be estimated; the peak area intensity ratio I_{F3}/I_{F4} is nearly 1.5, indicating that almost 60% of the amorphicity seen for inorganic polymer G80 is due to the presence of glass.

ORM analysis

Figures 4 and 5 show polarized microscope pictures for slag–glass (SG80) and glass-based (G80) inorganic polymers, respectively. In Fig. 4 where parallel Nicols are used,

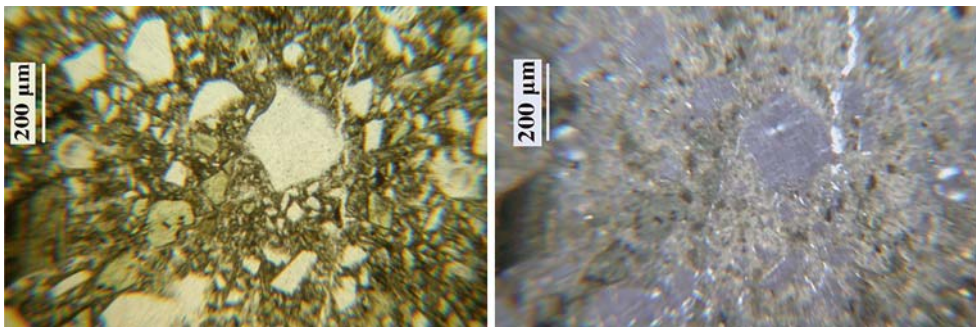

Fig. 4 Polarized microscope (scale 200 μm) pictures for slag–glass inorganic polymer (SG80), in parallel (*left*) and crossed Nicols (*right*)

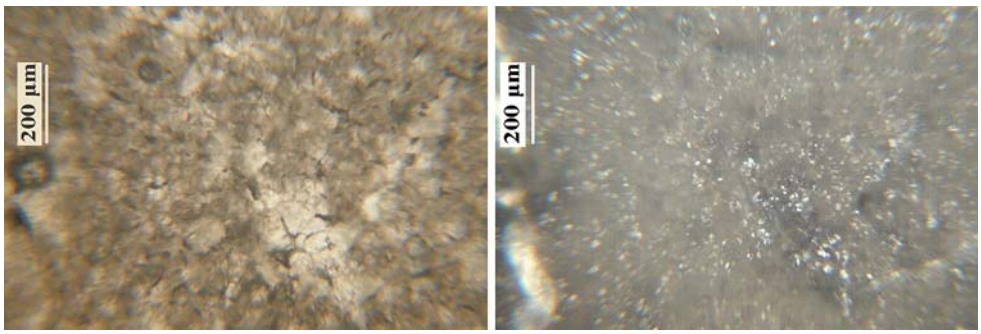

Fig. 5 Polarized microscope (scale 200 μm) pictures for glass-based inorganic polymer (G80), in parallel (*left*) and crossed Nicols (*right*)

angular white glass grains with varying dimensions are seen; when Nicols are crossed glass grains become dark due to isotropy and amorphicity. Slag grains are dispersed in inorganic polymer gel and cannot be easily seen. The high compressive strength acquired (52 MPa) for SG80 inorganic polymer is due to the high content of glass in the starting mixture.

The amorphicity of inorganic polymer G80 is obvious as seen in Fig. 5; no glass grains are detected and the gel formed is quite homogenous. The result of high amorphicity and homogeneity is confirmed by the superior strength acquired reaching 125 MPa.

The bright areas seen in pictures taken using crossed Nicols (Figs. 4, 5) indicate the presence of crystalline phases or anisotropic materials. These phases may be trona or pirssonite, which are formed at the surface of inorganic polymers some time after synthesis as a result of atmospheric carbonation.

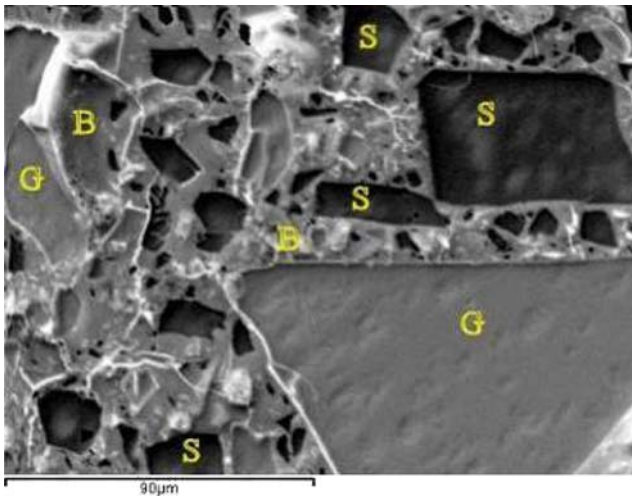

Fig. 6 SEM-BSI of inorganic polymer SG80 (*G* glass grains, *S* slag grains, *B* gel), scale 90 μm [34]

SEM analysis

A backscattered electron image (BSI) displaying the morphology of a 50%–50% w/w slag–glass inorganic polymer (SG80) is shown in Fig. 6. The matrix is quite heterogenous; slag and glass grains are clearly seen (slag grains are darker). The inorganic polymer gel is seen between slag and glass grains and acts as a binder enhancing thus the compressive strength of the specimen.

The element spectrum of a slag grain consists mainly of silicon, iron, aluminium and calcium, whilst some chromium, magnesium and potassium are also present. Glass grains contain silicon and some calcium and magnesium. Figure 7 shows the element spectrum of gel for specimen SG80. The gel consists of silicon and aluminium solubilized from the raw materials; silicon is also provided from the sodium silicate solution used as activator during synthesis. The Si/Al ratio in gel ($\sim$13) is bigger than the respective ratio in slag ($\sim$3) and lower than that in glass ($\sim$19). The Si/Al ratio is highly affected by the potassium hydroxide concentration which controls the dissolution of Si and Al from raw materials.

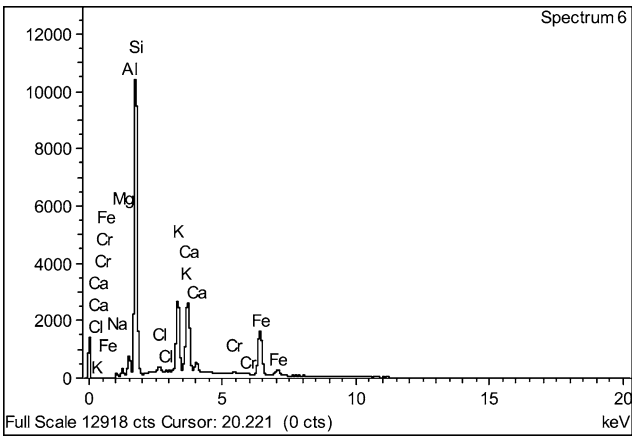

Fig. 7 Element spectrum of inorganic polymer SG80 gel seen in Fig. 6

Considering that Si and Ca are the main elements present in gel (Ca/Si = 0.3) it is assumed that calcium participates in the formation of Ca polysialate-(di)siloxo structures or calcium silicate hydrates (CSH). However, these CSH phases differ from those formed during hydration of Portland cement and have higher calcium content (Ca/Si = 1.6) [31–33].

Iron and some chromium solubilized from slag are also seen in the element spectrum of inorganic polymer SG80 gel (Fig. 7). This implies that solubilization takes place even at relatively low temperatures (<80 °C) and both elements are bound in gel. The Fe/Cr ratio is almost identical both in slag and gel (~7) indicating that the dissolution rate of iron and chromium phases present in slag is pretty similar [34].

Figure 8 shows a backscattered electron image of a glass-based inorganic polymer (G80); the matrix is more homogenous than the one seen in Fig. 6. Glass grains are denoted by "*A*" and "*B*" while gel ("*C*" and "*E*") fills the area between them. "*D*" with a Si/Ca ratio of ~5 is an area consisting of Ca and Si rich phases. Elemental mapping (data not shown) proves the presence of silicon in glass grains and particularly in gel. Glass grains do not contain potassium and can be easily distinguished from gel which contains considerable amounts of potassium due to the use of KOH during synthesis. The Si/Al ratio in G80 gel (Fig. 9) is bigger (~45) than that in commercial glass (~19); additional Si ions were provided from sodium silicate solution used as activator.

FTIR analysis

Figure 10 shows the FTIR spectra of slag, glass as well as inorganic polymers G80 and SG80. The bands at 460–465 cm^{-1}, seen for slag and especially for glass and specimens G80 and SG80, are due to in plane Si–O

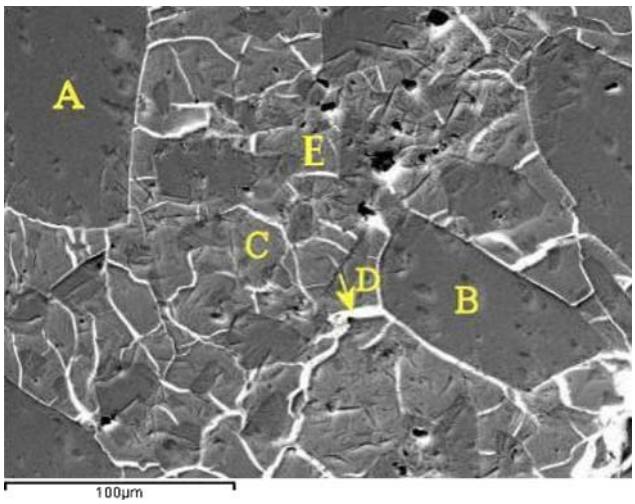

Fig. 8 SEM-BSI of inorganic polymer G80 (*A* and *B* glass grains, *C* and *E* gel, *D* Ca and Si rich phases), scale 100 µm

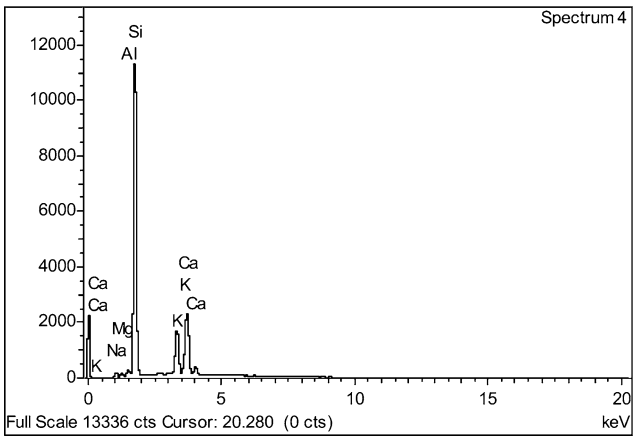

Fig. 9 Element spectrum of inorganic polymer G80 gel seen in Fig. 8

bending and Al–O linkages [35]. The small band seen at ~530 cm^{-1} only for the glass-based inorganic polymer (G80) is mainly due to out of plane Si–O bending [36]. A band identified at ~763 cm^{-1} for glass and G80 specimens is attributed to symmetric Si–O–Si and Si–O–Al stretching [37].

The band at around 1002 cm^{-1} may be due to T–O–Si (T: Si or Al) asymmetric stretching vibration (950–1200 cm^{-1}) as a result of TO_4 reorganization that takes place during synthesis [30, 38]. The position of the bands depends on the length as well as the angle of the bonds in the silicate network; when aluminium is incorporated in the network the intensity of the band decreases [18, 38, 39]. All bands at around 1000 cm^{-1} are a major fingerprint of the inorganic polymeric matrix and define the extent of polysialation or aluminium incorporation [30]. The very strong peaks seen at ~1002 cm^{-1} (as well as at ~ 458 cm^{-1}) are assigned to long chain bonds and/or the excess of Al–Si gel formed [12].

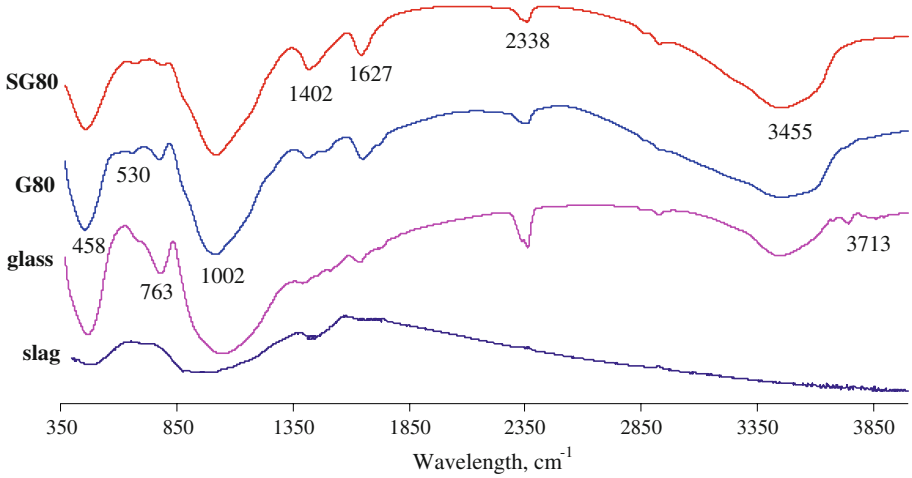

Fig. 10 FTIR spectra of slag, glass and inorganic polymers G80 και SG80

Atmospheric carbonation is evident at the region of 1410–1570 cm^{-1}; part of the excess Na present in the matrix is carried to the surface where it reacts with carbon dioxide [40, 41]. The band seen at 1627 cm^{-1} for glass and inorganic polymers is attributed to bending vibrations (H–O–H) and is typical for polymeric structures with aluminosilicate networks [37, 42]. Stretching vibrations of the bond –OH are seen at 3200–3600 cm^{-1} due to the weak bonds of H_2O molecules absorbed on the surface or bonded into inorganic polymer gel; the exact position of the bond –OH depends on the strength of the bond [12, 36, 37]. The small bands seen at around 2400 cm^{-1} are probably due to the infrared band position of HCO_3^- ions [36].

In conclusion, various infrared absorption bands may be used for the identification of bonds such as Si–O, Al–O and T–OH in the inorganic polymer structure. These bonds are formed when slag and glass react with the activating solution and solubilization of elements takes place. Stretching vibrations of the bond T–O–Si seen between 950–1200 cm^{-1} indicate the formation of gel during polycondensation.

TG analysis

Figure 11 shows TG curves for inorganic polymers G80 and SG80; for both specimens the initial weight used was 100 mg. The total calculated weight loss is 12.3% and 8.6% w/w, respectively. The absorbed water is lost at temperatures less than 100 °C; increase of temperature results in shrinkage and finally damage of inorganic polymer structure [43, 44]. The remaining water is either bound tightly or is less able to diffuse to the surface and continues to evaporate slowly at higher temperatures [45]. The continuous weight loss up to almost 500 °C is due to evaporation of hygroscopic water or water residing in the channels [46]. Very limited weight loss is seen at higher temperatures indicating that no other reactions take place.

Since water is an important part of the final inorganic polymer structure ($M_n((SiO_2)_z–AlO_2)_n \cdot wH_2O$), an adequate water content should be present in the initial inorganic polymer paste so that reactions proceed, a substantial quantity of gel is formed and a noticeable compressive

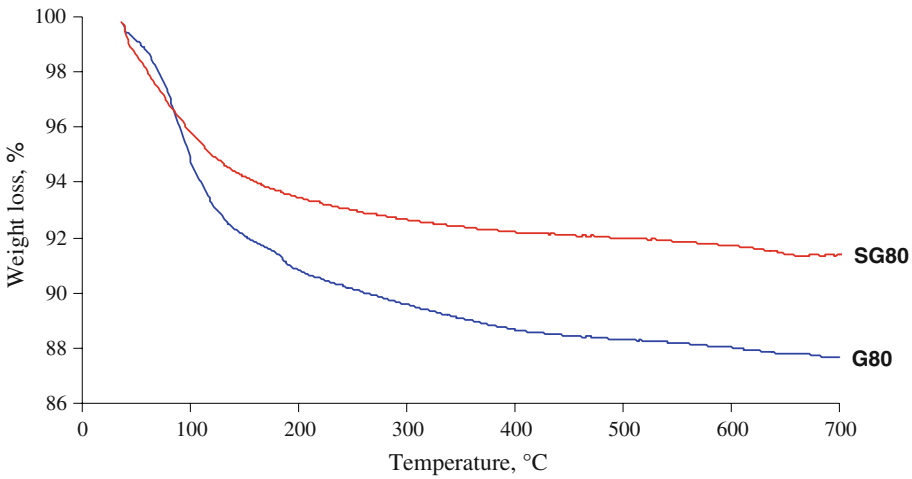

Fig. 11 TG curves of weight versus temperature for inorganic polymers G80 and SG80

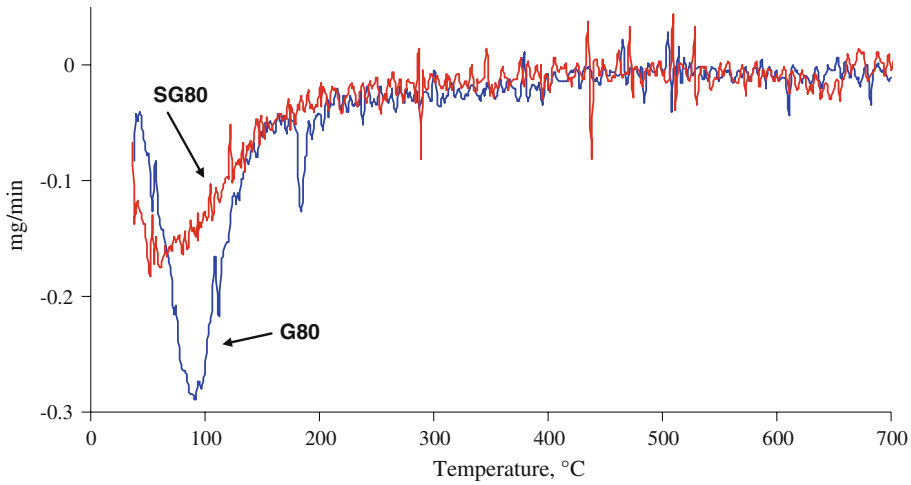

Fig. 12 DTG curves of rate of weight loss versus temperature for inorganic polymers G80 and SG80

strength is acquired; a short pre-curing period (1–2 days) may by extremely beneficial in this case [27, 47].

DTG thermograms are presented in Fig. 12; the noise seen in some parts of the curves is due to instrumental difficulties. All curves are typical of poly(sialate-siloxo) inorganic polymers. The endotherms seen at approximately 100 °C can be attributed to evaporation of free pore water that results in slight increase of porosity [48, 49]. The appearance of a distinct minimum in the dehydration endotherm for specimen G80 implies that more water evaporates over this narrow temperature range; this observation confirms the weight loss seen in Fig. 11. Moreover, the wider temperature span of the endotherm for specimen SG80 suggests that water is tightly bound in gel due to the presence of zeolitic phases that can easily incorporate water into their cage-like structure [48].

Effect of the presence of heavy metals and anions in the starting mixture on gel quality

Pb and Cu were added as sulphate and nitrate salts in the starting mixture in order to study the effect of the presence of heavy metals and anions on gel quality and subsequently on the compressive strength of the inorganic polymers produced.

Addition of 0.5–3% w/w Pb as $Pb(NO_3)_2$ or $PbSO_4$ in slag-based inorganic polymers results in a decrease of the compressive strength up to 70%. Addition of Cu as nitrate or sulphate salt results in a gradual decrease of the compressive strength but when the addition percentage exceeds 2% w/w no inorganic polymer structure is formed and no strength is acquired. It has been shown that presence of both metals as sulphate salts has a less negative effect on inorganic polymer structure.

NO_3^- and SO_4^{2-} ions present in solution react and consume part of the activating KOH solution reducing thus its effect in raw materials dissolution and the volume of inorganic polymer gel formed. Reactions (3) and (4) are indicative reactions involving lead sulphate and copper nitrate, respectively.

$$2KOH + PbSO_4 + 3Na_2SiO_3 \rightarrow Na_6PbO_5 + K_2SO_4 + 3SiO_2 + H_2 \quad (3)$$

$$2KOH + Cu(NO_3)_2 \cdot 3H_2O + Na_2SiO_3 \rightarrow Cu(OH)_2 + 2K(Na)NO_3 + SiO_2 + 3H_2O \quad (4)$$

According to reaction (3), a small amount of Pb reacts and is bound as Na_6PbO_5 which is a low solubility phase. It seems that some Pb is immobilized in the amorphous phase of inorganic polymer PBN3 since this specimen acquires a relatively high compressive strength of 16 MPa. On the contrary no Cu seems to react and form stable phases as indicated in reaction (4).

Figure 13 shows the evolution of the compressive strength of slag-based inorganic polymers PBN, PBS, CUN and CUS in relation with the percentage of consumed KOH moles, under the assumption that all present anions react with KOH. It is seen from this figure that the compressive strength drops substantially when a certain percentage of available KOH moles have reacted with either NO_3^- or SO_4^{2-} ions. However, it is important to underline that the number of NO_3^- or SO_4^{2-} ions in solution depends on the type of salt added. For example, when 3% w/w Pb is added as $Pb(NO_3)_2$ in the starting mixture approximately 6 g of NO_3^- ions are present in solution; on the other hand, addition of the same percentage of Pb as a sulphate salt results in the presence of 4.5 g of SO_4^{2-} ions. It is deduced therefore that in the case of nitrates more available moles KOH are consumed (specimens PBN and CUN) and therefore less moles of KOH participate in gel synthesis reactions [47].

It is seen from the experimental data that the presence of anions such as NO_3^- or SO_4^{2-} even in low concentrations in the starting mixture has a more detrimental effect on gel

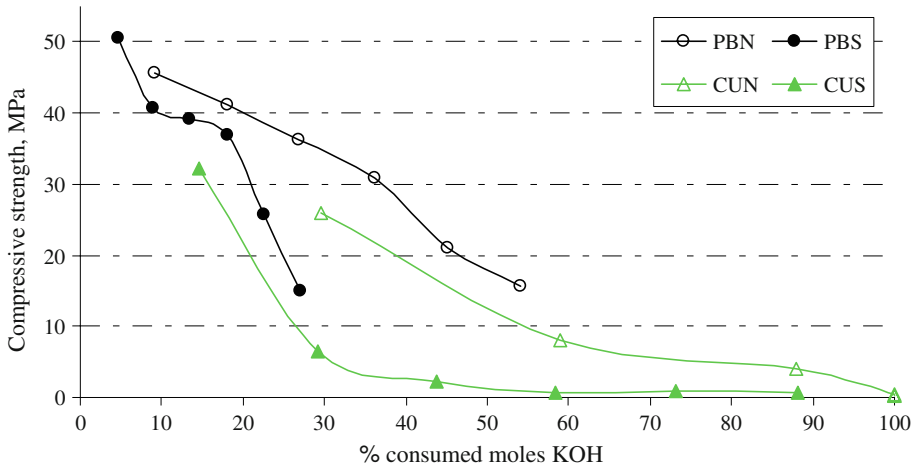

Fig. 13 Compressive strength of inorganic polymers PBN, PBS, CUN and CUS in relation with the percentage of KOH moles reacted with NO_3^- or SO_4^{2-} ions

formation and hardening and subsequently on the compressive strength of inorganic polymers than the presence of heavy metals such as Pb and Cu, which are encapsulated and immobilized in the gel formed; this is an issue though that requires a more thorough investigation with the use of advanced analytical techniques.

Conclusions

The results of this experimental study show that the use of analytical techniques, namely XRD, ORM, SEM, FTIR and TG offer significant insights pertinent to the identification of the composition of gel and the mechanisms involved during synthesis of inorganic polymers, when low calcium ferronickel slag and commercial slag are used as raw materials and KOH and Na_2SiO_3 as activating solutions.

XRD provides useful information regarding new formed phases such as hydroxysodalite, maghemite, calcite, calcium silicate hydrated phases and trona. The formation of new phases enables the prediction of reactions between raw materials and activating solutions. Deconvolution of the amorphous peaks in XRD patterns enables the quantitative estimation of the degree of amorphicity, which reaches 60% for glass-based specimens.

Optical reflection microscopy (ORM) gives some information regarding presence of crystalline phases or anisotropic materials in inorganic specimen structure, shape and dimensions of crystals, as well as to a certain degree amorphicity and homogeneity of the gel formed.

In addition to ORM, SEM can be used to fully identify the morphology of inorganic polymers and the chemistry of the grains in order to assess the extent of dissolution of the raw materials as well as the role of the activating solutions used. Furthermore, SEM provides very important data pertinent to the quality of the gel (ratios Si/Al, Ca/Si and Fe/Cr, presence of CSH phases) and the strength of inorganic polymers, enabling thus the identification of reactions and mechanisms involved in the process.

Fourier transform infrared spectroscopy (FTIR) provides major fingerprints for the inorganic polymeric matrix, through identification of specific molecular structures such as Si–O, Si–O–Si or Al–O–Si that define the degree of polysialation and the extent or aluminium incorporation; it also provides information regarding the quality of the gel formed as well as whether any atmospheric carbonation takes place.

TG/DTG may be used to determine water evaporation rates and predict potential shrinkage and damage of inorganic polymer structure under specific heating conditions. Adequate water content should be present in the starting paste so that gel forming reactions proceed well and a noticeable compressive strength is acquired; these are induced by considering a short pre-curing period.

The use of analytical techniques provides useful information regarding quality, morphology and characteristics of the gel formed. This data may be used to elucidate reactions involving raw materials and activating solutions as well as prevailing inorganic polymer synthesis mechanisms.

Finally, it is seen that the presence of anions such as NO_3^- or SO_4^{2-} in the starting mixture has a more detrimental effect on gel formation and hardening and subsequently on the compressive strength of inorganic polymers than the presence of heavy metals such as Pb and Cu. These anions consume available moles of the activating solution and therefore the gel formed is not of sufficient quantity and adequate quality to encapsulate and immobilize the heavy metals present.

Acknowledgements The authors would like to acknowledge the financial support of the Research Committee of Technical University Crete for the basic research project "Elucidation of mechanisms of immobilization of heavy metals during inorganic polymer synthesis using ferronickel slag" as well as LARCO S.A. for providing the slag.

References

1. Davidovits J (1988) In: Davidovits J, Orlinski J (eds) Proceedings of the 1st international conference geopolymer '88, vol 1. Compiegne, France, pp 19–23
2. Duxson P, Fernández-Jiménez A, Provis JL, Lukey GC, Palomo A, Van Deventer JSJ (2007) J Mater Sci 42:2917. doi:10.1007/s10853-006-0637-z
3. Davidovits J (1984) US Patent 4,472,199
4. Cioffi R, Maffucci L, Santoro L (2003) Resour Conserv Recyl 40(1):27
5. Van Jaarsveld JGS, Van Deventer JSJ, Schwartzman A (1999) Miner Eng 12(1):75
6. Phair JW, Van Deventer JSJ (2002) Int J Miner Process 66(1–4):121
7. Astutiningsih S, Liu Y (2005) In: Davidovits J (ed) Proceedings of the world congress geopolymer. Saint Quentin, France, p 69
8. Van Deventer JSJ, Provis JL, Duxson P, Lukey GC (2007) J Hazard Mater A139(3):506
9. Provis JL, Yong CZ, Duxson P, Van Deventer JSJ (2009) Colloids Surf A 336:57
10. Davidovits J, Comrie DC, Paterson JH, Ritcey DJ (1990) Concr Int 12(7):30
11. Bakharev T, Sanjayan JG, Chen Y-B (2003) Cem Concr Res 33(10):1607
12. Bakharev T (2005) Cem Concr Res 35:1224
13. Davidovits J (1988) In: Davidovits J, Orlinski J (eds) Proceedings of the 1st international conference on geopolymer '88, vol 1. Compiegne, France, pp 25–48
14. Comrie DC, Paterson JH, Ritcey DJ (1988) In: Davidovits J, Orlinski J (eds) Proceedings of the 1st international conference on geopolymer '88, vol 1. Compiegne, France, pp 107–123
15. Van Jaarsveld JGS, Van Deventer JGJ, Lorenzen L (1997) Miner Eng 10(7):659
16. De Silva P, Sagoe-Crenstil K (2008) Cem Concr Res 38(6):870
17. Simonsen ME, Sønderby C, Søgaard EG (2009) J Sol-Gel Sci Technol 50:372
18. Simonsen ME, Sønderby C, Li Z, Søgaard EG (2009) J Mater Sci 44(8):2079. doi:10.1007/s10853-009-3270-9
19. Zuhua Z, Xiao Y, Huajun Z, Yue C (2009) Appl Clay Sci 43:218
20. Xu H, Van Deventer JSJ (2000) Int J Miner Process 59(3):247
21. Komnitsas K, Zaharaki D (2007) Miner Eng 20:1261
22. Temuujin J, Van Riessen A, Williams R (2009) J Hazard Mater. doi:10.1016/j.jhazmat.2008.12.121
23. Zaharaki D, Komnitsas K, Perdikatsis V (2006) In: Agioutantis Z, Komnitsas K (eds) Proceedings of the 2nd international conference on advances in mineral resources management and environmental geotechnology. Chania, Crete, Greece, p 63
24. Temuujin J, Williams RP, Van Riessen A (2009) J Mater Process Technol 209(12–13):5276
25. Van Jaarsveld JGS, Van Deventer JSJ, Lukey GC (2004) Chem Eng Commun 191:531
26. Komnitsas K, Zaharaki D, Perdikatsis V (2007) J Mater Sci 42:3073. doi:10.1007/s10853-006-0529-2
27. Komnitsas K, Zaharaki D, Perdikatsis V (2009) J Hazard Mater 161:760
28. Barrer RM, Mainwaring DE (1972) J Chem Soc Dalton Trans 12:1254
29. Dombrowski K, Buchwald A, Weil M (2007) J Mater Sci 42:3033. doi:10.1007/s10853-006-0532-7
30. Gadsden A (1975) Infrared spectra of minerals and related inorganic compounds. Butterworths, London
31. Gani MSJ (1997) Cement and concrete, 1st edn. Chapman and Hall, London
32. Yip CK, Lukey GC, Van Deventer JSJ (2005) Cem Concr Res 35(9):1688
33. Zhang Y, Sun W, Chen Q, Chen L (2007) J Hazard Mater 143(1–2):206
34. Zaharaki D, Komnitsas K (2009) Global NEST Journal (in press)
35. Van Jaarsveld JGS, Van Deventer JSJ, Lukey GC (2002) Chem Eng J 89(1–3):63
36. Socrates G (2001) Infrared and raman characteristic group frequencies, 3rd edn. Wiley, England
37. Bakharev T (2005) Cem Concr Res 35(4):658
38. Rees CA, Provis JL, Van Lukey GC, Deventer JSJ (2007) Langmuir 23:8170–8179
39. Rees CA, Provis JL, Lukey GC, Van Deventer JSJ (2008) Colloids Surf A 318:97
40. Barbosa VFF, Mackenzie KJD, Thaumaturgo C (1999) In: Davidovits J, Davidovits R, James C (eds) Proceedings of the 2nd international conference geopolymere '99. Saint-Quentin, France, p 65
41. Barbosa VFF, MacKenzie KJD, Taumaturgo C (2000) Int J Inorg Mater 2:309
42. Mozgawa W, Deja J (2009) J Mol Struct. doi:10.1016/j.molstruc.2008.12.026
43. Kong DLY, Sanjayan JG (2008) Cem Concr Compos 30(10):986
44. Kong DLY, Sanjayan JG, Sagoe-Crentsil K (2008) J Mater Sci 43(3):824. doi:10.1007/s10853-007-2205-6
45. Subaer Van, Riessen A (2007) J Mater Sci 42(9):3117. doi:10.1007/s10853-006-0522-9
46. Perraki T, Kakali G, Kontori E (2005) J Therm Anal Calorim 82:109
47. Zaharaki D (2009) PhD thesis, Department of Mineral Resources Engineering, Technical University of Crete, Hania, Greece
48. Duxson P, Lukey GC, Van Deventer JSJ (2007) J Mater Sci 42:3044. doi:10.1007/s10853-006-0535-4
49. Perera DS, Uchida O, Vance ER, Finnie KS (2007) J Mater Sci 42:3099. doi:10.1007/s10853-006-0533-6